Geophysical Research Letters

RESEARCH LETTER
10.1029/2019GL084384

Early Holocene Temperature Oscillations Exceed Amplitude of Observed and Projected Warming in Svalbard Lakes

Willem G. M. van der Bilt[1,2], William J. D'Andrea[3], Johannes P. Werner[2], and Jostein Bakke[1,2]

[1]Department of Earth Science, University of Bergen, Bergen, Norway, [2]Bjerknes Centre for Climate Research, Bergen, Norway, [3]Lamont-Doherty Earth Observatory, Columbia University, New York, NY, USA

Abstract Arctic climate is uniquely sensitive to ongoing warming. The feedbacks that drive this amplified response remain insufficiently quantified and misrepresented in model scenarios of future warming. Comparison with paleotemperature reconstructions from past warm intervals can help close this gap. The Early Holocene (11.7–8.2 ka BP) is an important target because Arctic temperatures were warmer than today. This study presents centennially resolved summer temperature reconstructions from three Svalbard lakes. We show that Early Holocene temperatures fluctuated between the coldest and warmest extremes of the past 12 ka, exceeding the range of instrumental observations and future projections. Peak warmth occurred ~10 ka BP, with temperatures 7 °C warmer than today due to high radiative forcing and intensified inflow of warm Atlantic waters. Between 9.5 and 8 ka BP, temperatures dropped in response to freshwater fluxes from melting ice. Facing similar mechanisms, our findings may provide insight into the near-future response of Arctic climate.

Plain Language Summary The Arctic warms much faster than the global average. This amplified response can trigger feedbacks that affect the trajectory of future change. In areas formerly covered by ice, darker open water or rocks reflect less solar heat, enhancing warming. However, freshwater from melting ice may slow ocean circulation, leading to cooling. The climate impact of these mechanisms remain insufficiently understood, restricting efforts to predict future change. To reduce uncertainty, our research uses geological information from the most recent past period when the Arctic was warmer than the present, the Early Holocene, which lasted from 11,700 to 8,200 years ago. We analyzed fats from algae preserved in Svalbard lakes that yield information about past summer temperatures. Our findings show that the Early Holocene was characterized by the coldest and warmest extremes experienced since the last Ice Age. During peak warmth, summer temperatures were 7 °C warmer than today as more solar radiation and warm water reached the Arctic. However, Early Holocene warming was much slower than today. But warming was interrupted when freshwater pulses from melting Ice Sheets lowered temperatures. As we face a warmer Arctic with a melting Greenland Ice Sheet, our findings provide a rare window into the region's future.

Key Points:
- Temperatures exceeded instrumental and projected values ~10 ka BP as reinvigorating ocean circulation compounded radiative forcing
- Temperatures drop ~9.5–8 ka BP as the impact of freshwater from the melting Laurentide Ice Sheet overwhelms warming
- First terrestrial evidence from the Nordic Seas of surface cooling in response to the meltwater-driven 9.3 and 8.2 ka climate events

Supporting Information:
- Supporting Information S1

Correspondence to:
W. G. M. van der Bilt,
willemvanderbilt@uib.no

Citation:
van der Bilt, W. G. M., D'Andrea, W. J., Werner, J. P., & Bakke, J. (2019). Early Holocene temperature oscillations exceed amplitude of observed and projected warming in Svalbard lakes. *Geophysical Research Letters*, *46*, 14,732–14,741. https://doi.org/10.1029/2019GL084384

Received 2 JUL 2019
Accepted 2 DEC 2019
Accepted article online 3 DEC 2019
Published online 20 DEC 2019

1. Introduction

Anthropogenic warming affects the Arctic more strongly than any other region on Earth. Arctic land surface temperatures rise up to 4 times faster than the global average (Huang et al., 2017). The magnitude of this Arctic amplification is driven by several mechanisms that accentuate or dampen the direct impacts of radiative forcing (Goosse et al., 2018). These feedbacks include increases in heat absorption by an expanding area of ice-free waters (Screen & Simmonds, 2010) and weakening of poleward heat transport by the North Atlantic Current due to freshwater input from melting ice (Thornalley et al., 2018). The climate impacts of these mechanisms have, however, not been fully quantified. This knowledge gap is illustrated by the underestimation of recently observed Arctic warming by several climate models (Stroeve et al., 2012). Evaluating simulations against well-constrained paleoclimate records from warmer-than-present intervals will enable better representation of key amplifying processes in the Arctic climate system (Fischer et al., 2018). The Early Holocene (*Greenlandian*; 11.7–8.2 ka BP) is a key target for such exercises, because Arctic temperatures reached warmer-than-present values (Lecavalier et al., 2017; McFarlin et al., 2018) while freshwater from the melting Laurentide Ice Sheet (LIS) overpowered radiative forcing at times (Carlson & Clark, 2012). However, efforts to study Early Holocene climate to improve projections of future change are limited by the scarcity of quantitative paleoclimate records with the chronological control and

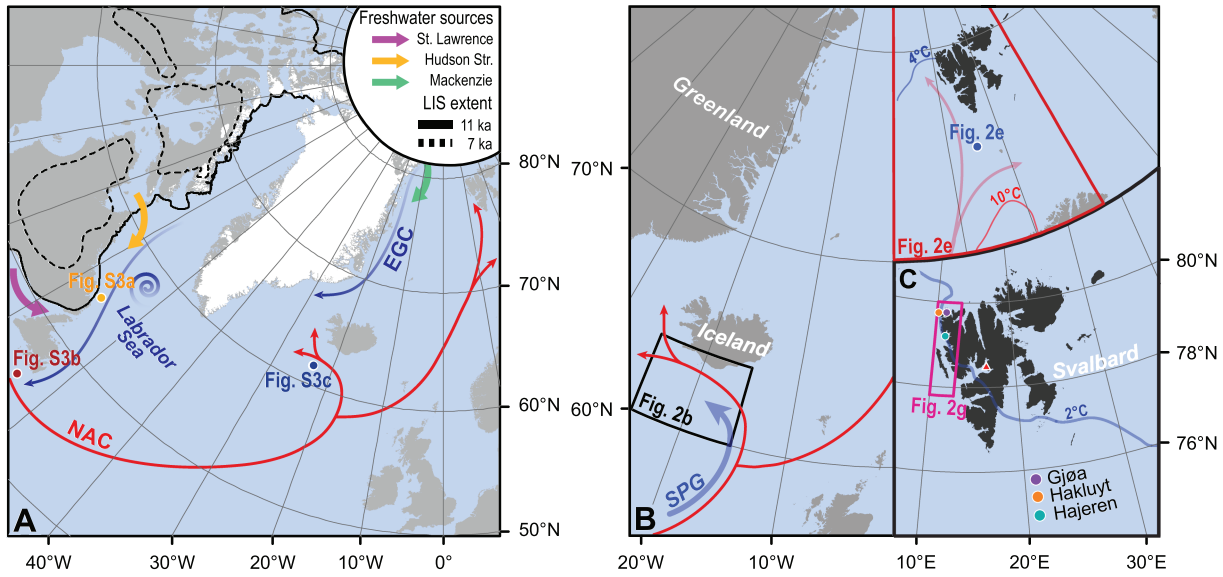

Figure 1. Maps of our study region and discussed records (dots) with figure references. (a) the North Atlantic with Laurentide ice extent (Dyke et al., 2003), meltwater pathways (arrows), ocean surface circulation (warm currents red, cool currents blue), and discussed records with figure references (colored dots). LIS, Laurentide Ice Sheet; NAC, North Atlantic Current; EGC, East Greenland Current; (b) the Nordic Seas with 4 °C (blue) and 10 °C (orange) August sea surface isotherms (Korablev et al., 2014), stacked overflow reconstructions from the Iceland-Scotland ridge (black rectangle; Thornalley et al., 2013), and the spatial extent of discussed summer temperature output from the LOVECLIM model (red trapezoid; Zhang et al., 2016). SPG, Subpolar Gyre; (c) Svalbard and the studied lakes with the CE 1979–2017 2 °C June-July-August (JJA) air temperature isotherm (blue line; Trouet & Van Oldenborgh, 2013), the extent of JJA air temperature output from the CMPIP5 ensemble (pink rectangle; Taylor et al., 2012), and the sampling area of *Z. crispata* molluscs (trapezoid; Mangerud & Svendsen, 2018).

sample density needed to resolve variability on human-relevant timescales (Sundqvist et al., 2014). Here, we discuss the pattern, magnitude, and causes of Early Holocene Arctic surface temperature change using three new reconstructions from Svalbard lake sediments. We rely on lacustrine alkenone unsaturation (U^K_{37}) from a known algal producer with an established temperature sensitivity to infer past growing season conditions (Longo et al., 2018). The presented records span the entire Holocene, placing variability in a 12 ka context, and resolve temperature change on centennial timescales.

2. Methods and Approach

We report Holocene-length temperature reconstructions from three lakes along the coast of northwest Spitsbergen. This area is particularly sensitive to climate change because of its proximity to the sea ice margin and the confluence of polar and Atlantic waters (Spielhagen et al., 2011). Our sites, Gjøavatnet (79.46°N,10.51°E), Hakluytvatnet (79.77°N,10.74°E), and Hajeren (79.26°N,11.52°E), were selected for their near-identical climatic setting (Figure 1c). They sit close to the seasonal sea ice margin, straddled along the 2 °C JJA (growing season) isotherm and at low (<50 m above sea level) elevation above the marine limit (Figure 1c) (Dee et al., 2011; Forman, 1990). However, differences do exist; importantly, glaciers drain into Gjøavatnet and Hajeren, while Hakluytvatnet is fed by snow melt. All lakes have been studied before; we sampled new material from previously collected cores and benefit from their undisturbed, often laminated, sedimentology and robust ^{14}C chronologies with sub-centennial resolution (Text S4 in the supporting information; De Wet et al., 2017; Gjerde et al., 2018; van der Bilt et al., 2015). We reconstruct Holocene growing season (June-July-August, JJA, in our study area; Text S2) surface (water) temperature variability using Long Chain Alkenones (LCAs) unsaturation, a paleothermometer that has shown great potential in Arctic lake sediments (e.g., D'Andrea et al., 2011). This study presents the first LCA data from Gjøavatnet (n = 98), and analyses of new samples from Hakluytvatnet (n = 35) and Hajeren (n = 11) (van der Bilt et al., 2016)—many in duplicate. Details about the extraction, saponification, separation, and measurement (uncertainty) of LCAs from sediment samples are outlined in Text S1. We rely on the widely used U^K_{37} index (Brassell et al., 1986) and fully resolve the tri-unsaturated isomers (Text S2; Longo et al., 2016). This allows chemotaxonomic identification of the alkenone producer, a key constraint on U^K_{37}-temperature sensitivity

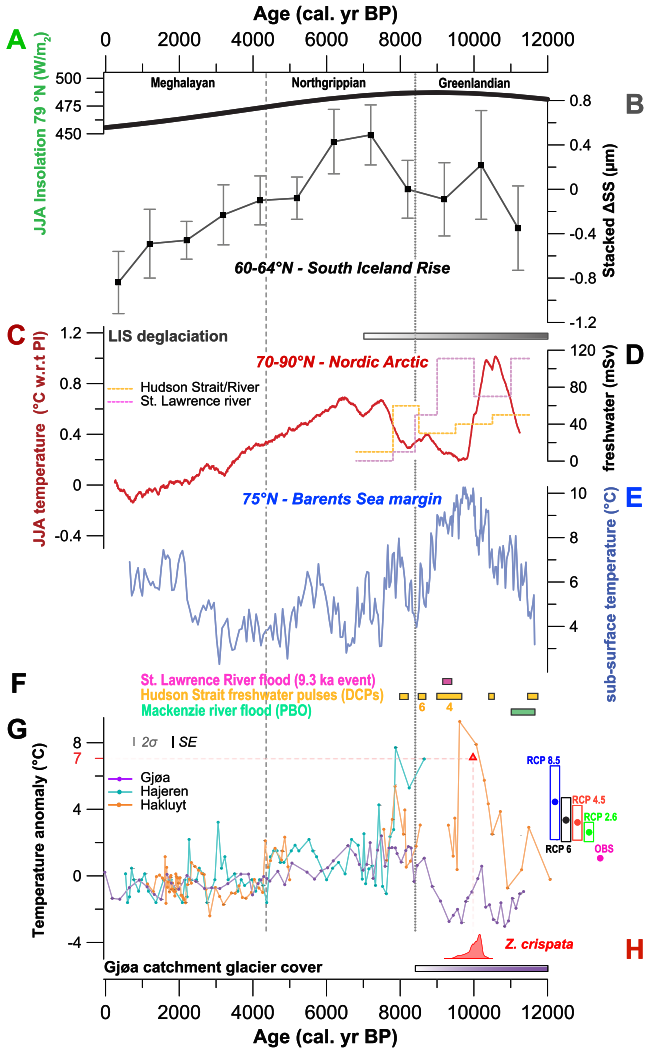

Figure 2. Selected regional Holocene paleoclimate records (color coding corresponds with Figure 1). (a) Summer (JJA) insolation at 79°N (Laskar et al., 2004); (b) stacked sortable silt-based (ΔSS) Iceland-Scotland overflow strength (Thornalley et al., 2013). (c) LOVECLIM-modeled JJA Svalbard preindustrial (PI) surface temperature anomalies (Zhang et al., 2016); (d) meltwater fluxes (stippled; Licciardi et al., 1999), and timing of LIS deglaciation (gray bar; Dyke et al., 2003); (e) Barents Sea margin subsurface summer temperatures (Risebrobakken et al., 2011); (f) the timing of major meltwater pulses (Clark et al., 2001; Jennings et al., 2015; Yu et al., 2010); (g) U^K_{37}-based PI temperature anomalies from studied lakes Gjøa, Hakluyt and Hajeren. We show no line when sample gaps exceed 2σ from the mean resolution; the absence of alkenones in Hakluytvatnet during the Northgrippian (8.2–4.2 ka BP) is due to a core hiatus. Bars on the right show the Q1–Q3 range of CE 2017–2100 JJA temperature scenarios from CMIP5 ensemble output for Svalbard (Text S4 and Figure 1c; Trouet & Van Oldenborgh, 2013). The vertical gray bar marks the analytical uncertainty (2σ) of measurements, while the black bar marks the reported SE of the applied U^K_{37} calibration by D'Andrea et al. (2016); (h) the summed probability of dated *Z. Crispata* molluscs (Mangerud & Svendsen, 2018) and August temperature requirements of this species (Text S4; red triangle). Bars at the bottom show when the Gjøa catchment was glaciarized (De Wet et al., 2017).

(D'Andrea et al., 2016), with the RIK_{37} and RIK_{38E} indices (Text S2 and Figure S1; Longo et al., 2016). We calibrated U^K_{37} values using the Group I phylotype regression of D'Andrea et al. (2016) that has been developed using in situ U^K_{37}-temperature data from Arctic lakes ($n = 10$, $r^2 = 0.94$, $p < 0.0001$). To compare our reconstructions to future simulations, we express alkenone-derived temperatures as anomalies from the CE 1850–1900 preindustrial (PI) baseline used by the Intergovernmental Panel on Climate Change (IPCC; Masson-Delmotte et al., 2018). To do so, our reconstructions were stacked and averaged using a hierarchy of Bayesian models (Text S3; Li et al., 2010).

3. Results and Discussion

3.1. The Imprint of Runoff From Local Glacier Melt on Reconstructed Temperatures

No alkenones were produced in Lake Hajeren prior to 8.6 ka BP, but the Gjøavatnet and Hakluytvatnet reconstructions identify the Early Holocene (*Greenlandian*; 11.7–8.2 ka BP) as the most dynamic epoch of the past 12 ka. As seen in Figure 2g, inferred temperatures range from colder to warmer than PI and present values, exhibiting a greater range of variability than seen over the past 8.2 ka BP. But while the Gjøa and Hakluyt records capture a similar pattern (Figure 2g), reflected by a maximum cross correlation of 0.46 ($n = 21$, $p = 0.06$) at a 300 year lag between evenly (100 year) resampled time series between 11.7 and 8.2 cal. ka BP, the baseline, amplitude and rate of change (RoC) differ. Reconstructed temperatures are colder and vary less in Gjøavatnet, especially during the warming peak centered on 10 ka BP (Figure 2g). The most apparent difference between these sites that could explain this offset is the sizable glacier (Annabreen) that drained into Gjøavatnet between ~11 and 10 ka BP (De Wet et al., 2017), while the Hakluyt catchment remained unglaciated (Gjerde et al., 2018). Input of cold meltwater from this body of ice might explain the suppressed temperature response in lake Gjøa. We evaluate this possibility using the XRF Ti-based reconstruction of Annabreen by De Wet et al. (2017) from the same core. Meltwater fluxes are determined by ice volume as well as ablation rates. On Svalbard, summer temperature presently controls the latter (Hagen et al., 2003). To determine this for the Early Holocene, we compare reconstructed summer temperatures from Hakluytvatnet, the nonglacial "control" lake, to variations in the activity of Annabreen in the Gjøa catchment. As seen in Figure 3a, temperature and glacier change display a strong inverse relationship: Warming coincides with less Ti-inferred glacier activity and cooling coincides with an increase in glacier activity. To investigate whether Annabreen meltwater fluxes can account for the offset between the Gjøa and Hakluyt reconstructions, we use the rate of glacier change (RoC, ΔTi counts per century; Text S4) as a surrogate for meltwater input. We account for the fact that larger glaciers produce greater volumes of meltwater by normalizing RoCs to (relative) size as reflected by XRF Ti counts after De Wet et al. (2017). As seen in Figures 2 and 3, the offset between the Gjøa and Hakluyt temperature reconstructions is largest when Annabreen is in retreat. Moreover, the onset of warming toward the optimum ~10 ka BP in Gjøa lags Hakluyt, but coincides with the highest retreat rates—suggesting that glacial melt delayed warming. Following the disappearance of Annabreen from the Gjøa catchment around 8.4 ka BP (De Wet et al., 2017), reconstructions from all three display a high degree of similarity (Figure 2g). Because of this convergence,

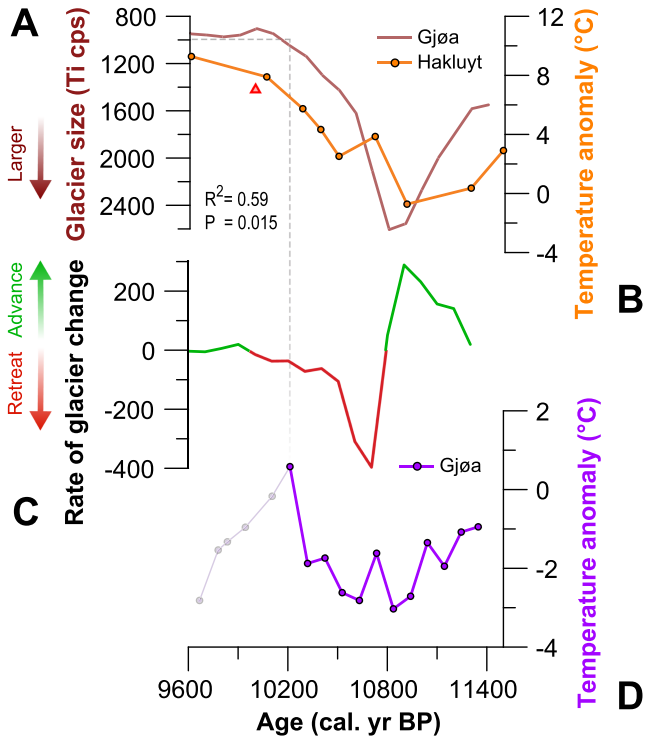

Figure 3. Linkages between reconstructed temperatures and glacier change during Early Holocene peak warming. (a) U^K_{37}-derived temperature anomalies from nonglacial Hakluytvatnet with the XRF Ti-based reconstruction of Annabreen glacier that feeds Gjøavatnet (De Wet et al., 2017). R^2 and P values highlight the strength of linear regression between both variables (X = U^K_{37}). The stippled line ~1,000 Ti counts marks when Annabreen glaciers is present but too small to exert significant influence on the lake after De Wet et al. (2017); (b) the RoC (Text S4) of Annabreen that highlight advances (green) and retreat (red); (c) U^K_{37}-derived temperature change from Gjøavatnet. Samples deposited when the influence of Annabreen became negligible (<1,000 Ti counts) are shown in lighter purple.

we solely used data from the Mid (*Northgrippian*) and Late (*Meghalayan*) Holocene to construct our temperature stack (Figure S2 and Text S3). Pearson correlation between this composite record and the Gjøa, Hajeren, and Hakluyt reconstructions at even (100 years) intervals respectively yield r^2 values of 0.66 ($n = 72$), 0.68 ($n = 77$) and 0.81 ($n = 36$) for the past 8 ka ($p < 0.001$). To assess the link between this shared response and Svalbard surface temperature change, we compared our stack to the Kongressvatnet record by D'Andrea et al. (2012). Uniquely, this U^K_{37}-based temperature reconstruction from a nearby lake on West Spitsbergen was validated using observations ($r^2 = 0.59$, $n = 15$, $p < 0.001$). Using the approach outlined in Text S3, Pearson correlation with our composite stack yields an R^2 value of 0.56 ($p = 0.015$). Following from the above, we are confident that our records capture a representative regional surface temperature signal.

3.2. Early Holocene Peak Warmth 10 ka BP: Radiative Forcing and Intensified Ocean Heat Advection Caused Warmer-Than-Present Conditions

Pronounced warming centered on 10 ka BP is one of the most distinct features in the presented records (Figure 2g). Particularly in Lake Hakluyt, which most sensitively captures surface temperate variability due to the absence of the influence of glacial meltwater (section 3.1). Here, our alkenone data indicate that growing season temperatures increased by ~7 °C between 10.5 and 9.5 ka BP and peaked at values that were up to 9 °C higher than the PI average. This is ~7 °C warmer than at present, using JJA observations from Svalbard for the CE 1912–2012 period as a reference period (Nordli et al., 2014). Supporting these findings, Mangerud and Svendsen (2018) derive a similar amplitude for peak Holocene warmth, based on the presence of *Zirfaea crispata*; a thermophilous mollusc that is not present in Svalbard waters today. The 10 °C August sea surface temperature isotherm in Figure 1b marks the present-day (CE 1900–2012) thermal limit of this boreal species (Korablev et al., 2014), 850 km south of the ~6 °C colder waters near our study area. As demonstrated by the summed probability distribution of dated Svalbard specimens ($n = 3$), the brief occurrence of *Z. Crispata* between 10.2 and 9.2 ka BP aligns with peak warmth in both Hakluyt and Gjøa records (Figure 2g). Comparing the near-identical estimates from alkenones and molluscs to emission scenarios, we find that the magnitude of warming is similar to CE 2017–2100 projections using a high emissions Representative Concentration Pathway (RCP) 8.5 (Figure 2g; Trouet & Van Oldenborgh, 2013). But while the amplitude of Early Holocene peak warmth may be analogous to near-future warming, RoCs are not. The pace of ongoing and projected warming is up to an order of magnitude faster than during the Early Holocene (Figure S2). Moreover, we cannot assume a proportional response between surface water and air temperatures (Text S2). Considering the mechanism(s) driving peak warmth around 10 ka BP (Figure 2), the broad contemporaneous summer insolation optimum cannot explain the rapid onset of warming. The inferred pattern of change is better explained by changes in ocean circulation. Simulations and reconstructions indicate abrupt phases of Atlantic Meridional Overturning Circulation reinvigoration and overshoot during glacial-interglacial transitions (Barker et al., 2010; Knorr & Lohmann, 2007), including the Earliest Holocene. During such episodes, large amounts of heat and salt that accumulated at lower latitudes throughout (glacial) phases of weakened overturning circulation, were rapidly advected northward. Risebrobakken et al. (2011) assessed this for the Early Holocene in the Nordic Seas south of Svalbard (Figure 1b), by reconstructing summer sea surface temperature change below the mixed layer to isolate the imprint of ocean heat from insolation-driven surface warming. As seen in Figure 2e, subsurface temperatures display a prominent peak around 10 ka BP that is unmatched in the remainder of the Holocene. Werner et al. (2015) infer a similar pattern of temperature change in the adjacent eastern Fram Strait. In addition, an IP_{25} reconstruction from the same site suggests

that the seasonal sea ice margin had retreated north of Svalbard at this time. As observed today, open water conditions are critical for the transfer of heat from ocean to atmosphere (Screen & Simmonds, 2010). Finally, stacked sortable silt-based reconstructions of deep water overflow from the Nordic Seas reveal that overturning circulation was not merely warmer but also more vigorous around 10 ka BP (Figure 2b; Thornalley et al., 2013), compared to previous and subsequent periods. Following from the above, we argue that a combination of radiative forcing, increased ocean heat advection and ice-free ocean waters resulted in summer temperatures that exceeded modern values on Svalbard ~10 ka BP. Placed in a regional context, our findings support a number of recent studies that suggest an earlier, warmer and more distinct Arctic Holocene optimum (Lecavalier et al., 2017; McFarlin et al., 2018). Collectively, this body of work stresses the need for data-model comparisons as simulations neither reproduce this reconstructed pattern nor its magnitude (Figure 2c; Zhang et al., 2018).

3.3. Cooler Conditions in Response to Gradual and Abrupt Freshwater Fluxes From the Melting LIS

Besides warmer-than-present conditions, the Early Holocene temperature history of northwest Spitsbergen was also marked by distinct cooling phases. Figure 2g shows that reconstructed temperatures repeatedly dropped below PI average values, especially in Gjøavatnet where meltwater from Annabreen glacier enhanced cooling until ~8.4 ka BP (De Wet et al., 2017). Set against a background of high radiative (insolation) forcing and ocean heat advection (Figures 2a, 2e; Laskar et al., 2004; Risebrobakken et al., 2011), as well as associated positive feedbacks in response to a lower albedo and restricted sea ice (Serreze & Barry, 2011), freshwater fluxes from melting ice sheets represent the most likely driver of cooling. During the Early Holocene (*Greenlandian*), disappearance of the LIS added 25–35 m to global sea level rise (Carlson et al., 2008). The cooling effects stemming from ensuing meltwater input resulted in changes in ocean heat advection, surface albedo and atmospheric circulation (e.g., Carlson & Clark, 2012; Kaufman et al., 2004; Sejrup et al., 2016). However, the spatiotemporal expression of these changes, as well as the sensitivity to gradual conditioning versus abrupt drainage, remains poorly constrained in time and space (Jennings et al., 2015).

3.3.1. Abrupt Cooling 11 ka BP: Ocean Freshwater Lid Triggered Short-Lived Climate Deterioration During the PBO

The first major Early Holocene cooling episode is centered on ~11 ka BP and marked by a ~3.5 °C growing season temperature decline in non-glacial Hakluytvatnet (Figure 2g). As seen in Figure 2f, the onset of cooling correlates firmly with the timing of abrupt LIS meltwater drainage through the Mackenzie river (Figure 1a), constrained by ^{14}C-dated flood deposits (Fisher et al., 2002) .This catastrophic flood has been linked to the preboreal oscillation (PBO), a climate interval with cooler summers in Greenland (~2°C) and Atlantic Europe (~1°C) (Heiri et al., 2004; Rasmussen et al., 2007). The high amplitude of inferred cooling on Svalbard (~3.5 °C) can be explained by the archipelago's proximity to meltwater routing. During the PBO, meltwater drained through the adjoining Fram Strait as other pathways were glaciated (Nares Strait) or dry (Bering Strait) (Figure 1a) (Dyke et al., 2003). Nearby marine records also capture a strong imprint of freshwater in our study area. Rasmussen et al. (2014) present evidence for cooling, freshening and stratification on the western Spitsbergen shelf. In addition, Bartels et al. (2017) observe that these changes were most pronounced at Svalbard sites that fringe the Arctic basin, where meltwater was confined before export through the Fram Strait. In summary, we argue that meltwater impacted Svalbard surface temperatures during the PBO by capping surrounding seas with a cold low-density lid, which inhibited the transfer of subsurface heat to the atmosphere.

3.3.2. Cooling 9.5–8 ka BP: Sustained Ice Sheet Melt Weakened Ocean Circulation and Triggered Positive Sea Ice Feedbacks

Following the PBO, temperatures increased and peaked ~10 ka BP (section 3.2), before a sharp decline ushered in a cold phase until ~8 ka BP (Figures 2g and S3). As highlighted in Figure S3, cooling appears to be more abrupt in Hakluytvatnet than Gjøavatnet. We tentatively attribute this divergence to differences in chronological and sampling resolution; as highlighted by the width of the bars in Figure S3d, the Gjøa record is better constrained in time during this interval. Also, as before (section 3.1), the magnitude of temperature change differs between records. While offsets narrow after peak glacier melt in the Gjøa catchment after 10 ka BP (Figure 2g; section 3.1), reconstructed temperatures remain higher in non-glacial Hakluytvatnet. However, at least for intervals covered by both records (we detected no alkenones in Hakluytvatnet from

9.3 to 8.5 ka BP), a similar pattern of change hints at a common response to the same forcing. After 10 ka BP, meltwater fluxes increased as LIS surface mass balance rapidly became more negative (Ullman et al., 2015). Also, as ice retreated north of the Great Lakes and into Hudson Bay, runoff was suddenly rerouted eastward through the St. Lawrence River and Hudson Strait (Figures 1a and 2d). As a result, large volumes of freshwater were released in a sensitive area where it could impact key components of the Atlantic Meridional Overturning Circulation: the Labrador Sea—a source of deep water formation (Pickart et al., 2002), the Subpolar Gyre—modulating the inflow of Atlantic water into the Nordic Seas (Hátún et al., 2005), and the North Atlantic Current—the main conduit for poleward surface ocean heat advection (Figures 1a and 1b; Rossby, 1996). Over millennial timescales, our temperature reconstructions mimic the pattern of the modeled surface response to sustained meltwater forcing in the Nordic Arctic by Zhang et al. (2016) (Figure 2f). The employed LOVECLIM Earth system model exhibits a high sensitivity of deep water formation near Svalbard to LIS freshwater input (Blaschek & Renssen, 2013). This is supported by empirical data; a decline in sortable silt grain size marks a decrease in deep water overflow across the Iceland-Scotland Ridge between ~10 and 8 ka BP (Figures 1b and 2b; Thornalley et al., 2013). In the simulation by Zhang et al. (2016), meltwater fluxes have been parameterized after Licciardi et al. (1999) and derive from gradual melt-driven runoff through the St. Lawrence River and, to a lesser extent, Hudson Strait (Figures 1a and 2d). δ^{18}O-based salinity reconstructions from the Laurentian Fan, located downstream from these pathways, reveal significant and sustained surface ocean freshening between 10 and 8 ka BP (Figures 1a and S3b (Keigwin et al., 2005). Yet proxy records of surface ocean conditions around Svalbard show no imprint of cool and fresh meltwater at the time. Even more so, Rasmussen et al. (2014) and Werner et al. (2015) collate evidence for widespread warm, ice-free and well-ventilated conditions. In this respect, we should note that LOVECLIM simulates the greatest reductions of deep water formation in winter (Thornalley et al., 2013). As shown by Longo et al. (2016), the onset of alkenone-producing haptophyte blooms is closely linked to the timing of lake ice melt (also see Text S2). While mostly controlled by growing season conditions, ice-off dates are also affected by the severity of the foregoing winter (Brown & Duguay, 2010). Following from the above, we argue that our reconstructions also capture persistent shifts in wintertime conditions.

Because of year-round mixing and heat advection, proxies used to characterize regional surface ocean conditions are less susceptible to this seasonal legacy effect (e.g., Risebrobakken et al., 2011). A notable exception are dinocysts, which record a more integrated seasonal signal (Matthiessen et al., 2005). Indeed, dinocyst-based temperature, sea ice, and salinity records indicate more severe and variable conditions in the Barents Sea, Fram Strait, and Greenland Sea, where anomalies were most extreme (de Vernal et al., 2013; Falardeau et al., 2018). In support of this evidence, Jennings et al. (2011) show that the East Greenland Current (Figure 1a), the main conduit for Arctic North Atlantic sea ice export, strengthened between 9.5 and 8.1 ka BP. The LOVECLIM experiment by Zhang et al. (2016), which simulates a similar JJA surface temperature response over Svalbard as our alkenone records (Figure 2g), reproduces East Greenland Current strengthening. As outlined by Delworth et al. (1997), such a scenario results in a southward migration of the Polar Front. This is supported by depleted leaf wax hydrogen isotope ratios (δD) from Hakluytvatnet sediments, which indicate a greater influence of Arctic air between 9.1 and 8.5 ka BP (Balascio et al., 2016). We thus argue that sustained LIS melt weakened deep convection near Svalbard and triggered sea ice feedbacks between 9.5 and 8 ka BP, overwhelming radiative warming.

3.3.3. Temperature Minima Superimposed on 9.5–8 ka BP Cooling: The Imprint of the 9.3 and 8.2 ka Meltwater Events

Over centennial timescales, our reconstructions capture a series of short-lived temperature minima, superimposed on low-frequency cooling between 10 and 8 ka BP (Figures 2 and S3). These shifts cannot be explained by sustained meltwater input from gradual LIS melt (Figures 2c and 2d) (Licciardi et al., 1999; Zhang et al., 2016). Freshwater was, however, also abruptly delivered to the North Atlantic by a series of Glacial Lake Outburst Floods (GLOFs) that were routed through the St. Lawrence River and Hudson Strait (Figure 1a) (Carlson & Clark, 2012). The sampling resolution and age control of our reconstructions (Gjøavatnet in particular) provide a valuable opportunity to assess the sensitivity of regional climate to these events (Carlson & Clark, 2012). We do so by comparing the timing of GLOFs (*trigger*) to temperature minima in the Gjøa and Hakluyt records (*response*) (Figures 2f, 2g, and S3) (Clark et al., 2001; Jennings et al., 2015; Yu et al., 2010). As seen in Figure 2d, cooling between 9.6 and 9 ka BP coincided with a series of closely spaced meltwater pulses. Notably, within chronological uncertainties of both records, the broad

temperature minimum observed around 9.3 ka BP overlaps with the timing of two major GLOFs (Figures 2f and S3a). First, the release of 40,000 km^3 of water from moraine-dammed Lake Superior into the St. Lawrence River (Yu et al., 2010). And second, drainage of an ice-dammed lake into the Hudson Strait that distributed locally sourced carbonates (DCP 4; Figure 2f) into the Labrador Sea (Jennings et al., 2015). A reduction in deep water ventilation at the time, coeval with surface ocean freshening and cooling (Came et al., 2007), suggests that these meltwater events impacted hydrographic conditions throughout the subpolar Atlantic. In addition, evidence for synchronous cooling from three Greenland ice cores indicates a regional surface temperature response (Rasmussen et al., 2007). Yet, to our knowledge, we present the first evidence of a terrestrial response to this 9.3 ka event from the Nordic Seas region.

While Hakluytvatnet sediments do not contain alkenones throughout the 9.3–8.5 ka interval (Figures 2g and S3d), the Gjøavatnet record captures an punctuated temperature recovery. Warming appears synchronous with a decline in melt-driven run-off (Figure 2b; Licciardi et al., 1999). The waning influence of freshwater on regional climate is also recorded by surface salinification off eastern Canada (Figures 1a and S3b; Keigwin et al., 2005), and strengthening Iceland-Scotland Ridge bottom flow (Figures 1a, 2b, and S3c; Praetorius et al., 2008). The apparent offset with these records falls within the uncertainty range of the respective chronologies; contemporaneous marine reservoir ages remain poorly constrained owing to highly variable meltwater input and ocean turnover (Jennings et al., 2015). Warming at this time is, however, punctuated by a ~2 °C cooling, centered on 8.3 ka BP in both of our records (Figures 2g and S3d). The timing corresponds to the 8.2 ka event (Alley et al., 1997), a phase of climate deterioration that has been linked to the collapse of the LIS over Hudson Bay and the final drainage of glacial lake Agassiz (Barber et al., 1999). The latter is captured by DCP 6 in Figures 2f and S3a (Jennings et al., 2015), which overlaps with the onset of cooling on Svalbard. Based on evidence of severe cooling on Greenland (Rasmussen et al., 2007), and significant weakening of Atlantic overturning circulation (Kleiven et al., 2008), the 8.2 ka event is often regarded as the most prominent Holocene freshwater event. In this respect, we note that the amplitude of change in our Svalbard reconstructions is comparatively modest (Figure S3d). This may suggest that sustained runoff had a greater impact on Svalbard temperatures than abrupt drainage.

4. Conclusions

Alkenone (U^K_{37}) data show that Svalbard experienced summer temperatures both warmer and colder than today during the Early Holocene. Warmth was greatest around 10 ka BP, when temperatures were up to ~7 °C higher than present in response to high radiative forcing and intensified ocean heat advection. In agreement with a growing body of recent work (e.g., Lecavalier et al., 2017; McFarlin et al., 2018), these findings indicate an earlier and warmer Holocene Optimum in the High Arctic then previously suggested. Moreover, comparison with model output shows that the amplitude of warming was on par with 21st century emission scenarios, but that temperatures rose much slower than today. A denser and more evenly spread distribution of similar high-resolution reconstructions is needed to ascertain if this signal is representative for the wider region. Between 10 and 8 ka BP, temperatures declined in response to freshwater input into the North Atlantic from melting ice sheets. The sensitivity of regional climate to freshwater forcing is of relevance for a future Arctic, which will likely be impacted by increased melt of the Greenland ice sheet and enhanced runoff as the hydrological cycle intensifies (Bintanja & Selten, 2014; Shepherd et al., 2012).

Acknowledgments
This research was supported by the ECONORS Fast Track Initiative from the Centre for Climate Dynamics (SKD) and a MOMENTUM grant to W. B. W. J. D acknowledges support from the G. Unger Vetlesen foundation. The authors would like to thank Liam Edwards-Gaherty for his help with lab work, and Jan Mangerud and Hans Renssen for fruitful discussion. All samples are archived at the Lamont-Doherty Earth Observatory of Columbia University (LDEO). Data published in this paper are stored in the PANGAEA repository.

References

Alley, R. B., Mayewski, P. A., Sowers, T., Stuiver, M., Taylor, K. C., & Clark, P. U. (1997). Holocene climatic instability: A prominent, widespread event 8200 yr ago. *Geology*, *25*(6), 483–486.

Balascio, N. L., D'Andrea, W. J., Gjerde, M., & Bakke, J. (2016). Hydroclimate variability of High Arctic Svalbard during the Holocene inferred from hydrogen isotopes of leaf waxes. *Quaternary Science Reviews*, *183*, 177–187.

Barber, D. C., Dyke, A., Hillaire-Marcel, C., Jennings, A. E., Andrews, J. T., Kerwin, M. W., et al. (1999). Forcing of the cold event of 8,200 years ago by catastrophic drainage of Laurentide lakes. *Nature*, *400*(6742), 344–348. https://doi.org/10.1038/22504

Barker, S., Knorr, G., Vautravers, M. J., Diz, P., & Skinner, L. C. (2010). Extreme deepening of the Atlantic overturning circulation during deglaciation. *Nature Geoscience*, *3*(8), 567.

Bartels, M., Titschack, J., Fahl, K., Stein, R., Seidenkrantz, M.-S., Hillaire-Marcel, C., & Hebbeln, D. (2017). Atlantic Water advection vs. glacier dynamics in northern Spitsbergen since early deglaciation. *Climate of the Past*, *13*(12), 1717–1749. https://doi.org/10.5194/cp-13-1717-2017

Bintanja, R., & Selten, F. (2014). Future increases in Arctic precipitation linked to local evaporation and sea-ice retreat. *Nature*, *509*(7501), 479–482. https://doi.org/10.1038/nature13259

Blaschek, M., & Renssen, H. (2013). The Holocene thermal maximum in the Nordic Seas: The impact of Greenland Ice Sheet melt and other forcings in a coupled atmosphere–sea-ice–ocean model. *Climate of the Past*, *9*(4), 1629–1643.

Brassell, S. C., Brereton, R. G., Eglinton, G., Grimalt, J., Liebezeit', G., Marlowe, I. T., et al. (1986). Palaeoclimatic signals recognized by chemometric treatment of molecular stratigraphic data. *Organic Geochemistry*, *10*(4-6), 649–660. https://doi.org/10.1016/S0146-6380(86)80001-8

Brown, L. C., & Duguay, C. R. (2010). The response and role of ice cover in lake-climate interactions. *Progress in Physical Geography*, *34*(5), 671–704.

Came, R. E., Oppo, D. W., & McManus, J. F. (2007). Amplitude and timing of temperature and salinity variability in the subpolar North Atlantic over the past 10 ky. *Geology*, *35*(4), 315–318.

Carlson, A. E., & Clark, P. U. (2012). Ice sheet sources of sea level rise and freshwater discharge during the last deglaciation. *Reviews of Geophysics*, *50*, RG4007. https://doi.org/10.1029/2011RG000371

Carlson, A. E., LeGrande, A. N., Oppo, D. W., Came, R. E., Schmidt, G. A., Anslow, F. S., et al. (2008). Rapid early Holocene deglaciation of the Laurentide ice sheet. *Nature Geoscience*, *1*(9), 620–624. https://doi.org/10.1038/ngeo285

Clark, P. U., Marshall, S. J., Clarke, G. K., Hostetler, S. W., Licciardi, J. M., & Teller, J. T. (2001). Freshwater forcing of abrupt climate change during the last glaciation. *Science*, *293*(5528), 283–287.

D'Andrea, W. J., Huang, Y., Fritz, S. C., & Anderson, N. J. (2011). Abrupt Holocene climate change as an important factor for human migration in West Greenland. *Proceedings of the National Academy of Sciences*, *108*(24), 9765–9769.

D'Andrea, W. J., Theroux, S., Bradley, R. S., & Huang, X. (2016). Does phylogeny control U37K-temperature sensitivity? Implications for lacustrine alkenone paleothermometry. *Geochimica et Cosmochimica Acta*, *175*, 168–180.

D'Andrea, W. J., Vaillencourt, D. A., Balascio, N. L., Werner, A., Roof, S. R., Retelle, M., & Bradley, R. S. (2012). Mild Little Ice Age and unprecedented recent warmth in an 1800 year lake sediment record from Svalbard. *Geology*, *40*(11), 1007–1010.

de Vernal, A., Hillaire-Marcel, C., Rochon, A., Frechette, B., Henry, M., Solignac, S., & Bonnet, S. (2013). Dinocyst-based reconstructions of sea ice cover concentration during the Holocene in the Arctic Ocean, the northern North Atlantic Ocean and its adjacent seas. *Quaternary Science Reviews*, *79*, 111–121.

De Wet, G., Balascio, N. L., D'Andrea, W. J., Bakke, J., Bradley, R. S., & Perren, B. (2017). Holocene glacier activity reconstructed from proglacial lake Gjøavatnet on Amsterdamøya, NW Svalbard. *Quaternary Science Reviews*, *183*, 188–203.

Dee, D. P., Uppala, S. M., Simmons, A. J., Berrisford, P., Poli, P., Kobayashi, S., et al. (2011). The ERA-Interim reanalysis: Configuration and performance of the data assimilation system. *Quarterly Journal of the Royal Meteorological Society*, *137*(656), 553–597. https://doi.org/10.1002/qj.828

Delworth, T. L., Manabe, S., & Stouffer, R. J. (1997). Multidecadal climate variability in the Greenland Sea and surrounding regions: A coupled model simulation. *Geophysical Research Letters*, *24*(3), 257–260.

Dyke, A. S., Moore, A., & Robertson, L. (2003). *Deglaciation of North America*. Ontario, Canada: Geological Survey of Canada Ottawa.

Falardeau, J., de Vernal, A., & Spielhagen, R. F. (2018). Paleoceanography of northeastern Fram Strait since the last glacial maximum: Palynological evidence of large amplitude changes. *Quaternary Science Reviews*, *195*, 133–152.

Fischer, H., Meissner, K. J., Mix, A. C., Abram, N. J., Austermann, J., Brovkin, V., et al. (2018). Palaeoclimate constraints on the impact of 2 °C anthropogenic warming and beyond. *Nature Geoscience*, *11*(7), 474–485. https://doi.org/10.1038/s41561-018-0146-0

Fisher, T. G., Smith, D. G., & Andrews, J. T. (2002). Preboreal oscillation caused by a glacial Lake Agassiz flood. *Quaternary Science Reviews*, *21*(8-9), 873–878.

Forman, S. L. (1990). Post-glacial relative sea-level history of northwestern Spitsbergen, Svalbard. *Geological Society of America Bulletin*, *102*(11), 1580–1590.

Gjerde, M., Bakke, J., D'Andrea, W. J., Balascio, N. L., Bradley, R. S., Vasskog, K., et al. (2018). Holocene multi-proxy environmental reconstruction from lake Hakluytvatnet, Amsterdamøya Island, Svalbard (79.5°N). *Quaternary Science Reviews*, *183*, 164–176. https://doi.org/10.1016/j.quascirev.2017.02.017

Goosse, H., Kay, J. E., Armour, K. C., Bodas-Salcedo, A., Chepfer, H., Docquier, D., et al. (2018). Quantifying climate feedbacks in polar regions. *Nature Communications*, *9*(1), 1919. https://doi.org/10.1038/s41467-018-04173-0

Hagen, J. O., Kohler, J., Melvold, K., & Winther, J. G. (2003). Glaciers in Svalbard: Mass balance, runoff and freshwater flux. *Polar Research*, *22*(2), 145–159.

Hátún, H., Sandø, A. B., Drange, H., Hansen, B., & Valdimarsson, H. (2005). Influence of the Atlantic subpolar gyre on the thermohaline circulation. *Science*, *309*(5742), 1841–1844.

Heiri, O., Tinner, W., & Lotter, A. F. (2004). Evidence for cooler European summers during periods of changing meltwater flux to the North Atlantic. *Proceedings of the National Academy of Sciences*, *101*(43), 15,285–15,288.

Huang, J., Zhang, X., Zhang, Q., Lin, Y., Hao, M., Luo, Y., et al. (2017). Recently amplified arctic warming has contributed to a continual global warming trend. *Nature Climate Change*, *7*(12), 875–879. https://doi.org/10.1038/s41558-017-0009-5

Jennings, A., Andrews, J., Pearce, C., Wilson, L., & Ólafsdóttir, S. (2015). Detrital carbonate peaks on the Labrador shelf, a 13–7 ka template for freshwater forcing from the Hudson Strait outlet of the Laurentide Ice Sheet into the subpolar gyre. *Quaternary Science Reviews*, *107*, 62–80. http://www.sciencedirect.com/science/article/pii/S0277379114004090

Jennings, A., Andrews, J., & Wilson, L. (2011). Holocene environmental evolution of the SE Greenland Shelf North and South of the Denmark Strait: Irminger and East Greenland current interactions. *Quaternary Science Reviews*, *30*(7–8), 980–998. www.sciencedirect.com/science/article/pii/S027737911100031X

Kaufman, D. S., et al. (2004). Holocene thermal maximum in the western Arctic (0–180°W). *Quaternary Science Reviews*, *23*(5–6), 529–560. http://www.sciencedirect.com/science/article/pii/S0277379103002956, https://doi.org/10.1016/j.quascirev.2003.09.007

Keigwin, L. D., Sachs, J. P., Rosenthal, Y., & Boyle, E. A. (2005). The 8200 year BP event in the slope water system, western subpolar North Atlantic. *Paleoceanography*, *20*, PA2003. https://doi.org/10.1029/2004PA001074

Kleiven, H. K. F., Kissel, C., Laj, C., Ninnemann, U. S., Richter, T. O., & Cortijo, E. (2008). Reduced North Atlantic deep water coeval with the glacial Lake Agassiz freshwater outburst. *Science*, *319*(5859), 60–64.

Knorr, G., & Lohmann, G. (2007). Rapid transitions in the Atlantic thermohaline circulation triggered by global warming and meltwater during the last deglaciation. *Geochemistry, Geophysics, Geosystems*, *8*, Q12006. https://doi.org/10.1029/2007GC001604

Korablev, A., Baranova, O. K., Smirnov, A. D., Seidov, D., & Parsons, A. R. (2014). Climatological atlas of the Nordic Seas and northern North Atlantic.

Laskar, J., Robutel, P., Joutel, F., Gastineau, M., Correia, A., & Levrard, B. (2004). A long-term numerical solution for the insolation quantities of the Earth. *Astronomy & Astrophysics*, *428*(1), 261–285.

Lecavalier, B. S., Fisher, D. A., Milne, G. A., Vinther, B. M., Tarasov, L., Huybrechts, P., et al. (2017). High Arctic Holocene temperature record from the Agassiz ice cap and Greenland ice sheet evolution. *Proceedings of the National Academy of Sciences*, *114*(23), 5952–5957. https://doi.org/10.1073/pnas.1616287114

Li, B., Nychka, D. W., & Ammann, C. M. (2010). The value of multiproxy reconstruction of past climate. *Journal of the American Statistical Association*, *105*(491), 883–895.

Licciardi, J. M., Teller, J. T., & Clark, P. U. (1999). Freshwater routing by the Laurentide Ice Sheet during the last deglaciation. *Geophysical Monograph-American Geophysical Union*, *112*, 177–202.

Longo, W. M., Huang, Y., Yao, Y., Zhao, J., Giblin, A. E., Wang, X., et al. (2018). Widespread occurrence of distinct alkenones from Group I haptophytes in freshwater lakes: Implications for paleotemperature and paleoenvironmental reconstructions. *Earth and Planetary Science Letters*, *492*, 239–250. https://doi.org/10.1016/j.epsl.2018.04.002

Longo, W. M., Theroux, S., Giblin, A. E., Zheng, Y., Dillon, J. T., & Huang, Y. (2016). Temperature calibration and phylogenetically distinct distributions for freshwater alkenones: Evidence from northern Alaskan lakes. *Geochimica et Cosmochimica Acta*, *180*, 177–196. http://www.sciencedirect.com/science/article/pii/S0016703716300576

Mangerud, J., & Svendsen, J. I. (2018). The Holocene Thermal Maximum around Svalbard, Arctic North Atlantic; molluscs show early and exceptional warmth. *The Holocene*, *28*(1), 65–83.

Masson-Delmotte, V., Zhai, P., Pörtner, H., Roberts, D., Skea, J., Shukla, P., & Waterfield, T. (2018). Global warming of 1.5 °C. An IPCC special report on the impacts of global warming of 1.5 °C above pre-industrial levels and related global greenhouse gas emission pathways, in the context of strengthening the global response to the threat of climate change, sustainable development, and efforts to eradicate poverty. IPCC. *Sustainable Development, And Efforts to Eradicate Poverty*.

Matthiessen, J., de Vernal, A., Head, M., Okolodkov, Y., Zonneveld, K., & Harland, R. (2005). Modem organic-walled dinoflagellate cysts in Arctic marine environments and their (paleo-) environmental significance. *Paläontologische Zeitschrift*, *79*(1), 3–51.

McFarlin, J. M., Axford, Y., Osburn, M. R., Kelly, M. A., Osterberg, E. C., & Farnsworth, L. B. (2018). Pronounced summer warming in northwest Greenland during the Holocene and Last Interglacial. *Proceedings of the National Academy of Sciences*, *115*(25), 6357–6362. https://doi.org/10.1073/pnas.1720420115

Nordli, Ø., Przybylak, R., Ogilvie, A. E., & Isaksen, K. (2014). Long-term temperature trends and variability on Spitsbergen: the extended Svalbard Airport temperature series, 1898-2012. *Polar Research*, *33*(1), 21349. https://doi.org/10.3402/polar.v33.21349

Pickart, R. S., Torres, D. J., & Clarke, R. A. (2002). Hydrography of the Labrador Sea during active convection. *Journal of Physical Oceanography*, *32*(2), 428–457.

Praetorius, S. K., McManus, J. F., Oppo, D. W., & Curry, W. B. (2008). Episodic reductions in bottom-water currents since the last ice age. *Nature Geoscience*, *1*(7), 449.

Rasmussen, S. O., Vinther, B. M., Clausen, H. B., & Andersen, K. K. (2007). Early Holocene climate oscillations recorded in three Greenland ice cores. *Quaternary Science Reviews*, *26*(15), 1907–1914.

Rasmussen, T. L., Thomsen, E., Skirbekk, K., Ślubowska-Woldengen, M., Klitgaard Kristensen, D., & Koç, N. (2014). Spatial and temporal distribution of Holocene temperature maxima in the northern Nordic seas: Interplay of Atlantic-, Arctic-and polar water masses. *Quaternary Science Reviews*, *92*, 280–291.

Risebrobakken, B., Dokken, T., Smedsrud, L. H., Andersson, C., Jansen, E., Moros, M., & Ivanova, E. V. (2011). Early Holocene temperature variability in the Nordic Seas: The role of oceanic heat advection versus changes in orbital forcing. *Paleoceanography*, *26*, PA4206. https://doi.org/10.1029/2011PA002117

Rossby, T. (1996). The North Atlantic Current and surrounding waters: At the crossroads. *Reviews of Geophysics*, *34*(4), 463–481.

Screen, J. A., & Simmonds, I. (2010). The central role of diminishing sea ice in recent Arctic temperature amplification. *Nature*, *464*(7293), 1334–1337. https://doi.org/10.1038/nature09051

Sejrup, H. P., Seppä, H., McKay, N. P., Kaufman, D. S., Geirsdóttir, Á., de Vernal, A., et al. (2016). North Atlantic-Fennoscandian Holocene climate trends and mechanisms. *Quaternary Science Reviews*, *147*, 365–378. https://doi.org/10.1016/j.quascirev.2016.06.005

Serreze, M. C., & Barry, R. G. (2011). Processes and impacts of Arctic amplification: A research synthesis. *Global and Planetary Change*, *77*(1–2), 85–96. http://www.sciencedirect.com/science/article/pii/S0921818111000397

Shepherd, A., Ivins, E. R., A, G., Barletta, V. R., Bentley, M. J., Bettadpur, S., et al. (2012). A Reconciled Estimate of Ice-Sheet Mass Balance. *Science*, *338*(6111), 1183–1189. http://www.sciencemag.org/content/338/6111/1183.abstract, https://doi.org/10.1126/science.1228102

Spielhagen, R. F., Werner, K., Sorensen, S. A., Zamelczyk, K., Kandiano, E., Budeus, G., et al. (2011). Enhanced modern heat transfer to the Arctic by warm Atlantic water. *Science*, *331*(6016), 450–453. https://doi.org/10.1126/science.1197397

Stroeve, J. C., Serreze, M. C., Holland, M. M., Kay, J. E., Malanik, J., & Barrett, A. P. (2012). The Arctic's rapidly shrinking sea ice cover: A research synthesis. *Climatic Change*, *110*(3-4), 1005–1027.

Sundqvist, H., Kaufman, D. S., McKay, N. P., Balascio, N. L., Briner, J. P., Cwynar, L. C., et al. (2014). Arctic Holocene proxy climate database–new approaches to assessing geochronological accuracy and encoding climate variables. *Climate of the Past Discussions*, *10*(1), 1–63. https://doi.org/10.5194/cpd-10-1-2014

Taylor, K. E., Stouffer, R. J., & Meehl, G. A. (2012). An overview of CMIP5 and the experiment design. *Bulletin of the American Meteorological Society*, *93*(4), 485–498.

Thornalley, D. J., Blaschek, M., Davies, F. J., Praetorius, S., Oppo, D. W., McManus, J. F., et al. (2013). Long-term variations in Iceland–Scotland overflow strength during the Holocene. *Climate of the Past*, *9*(5), 2073–2084.

Thornalley, D. J., Oppo, D. W., Ortega, P., Robson, J. I., Brierley, C. M., Davis, R., et al. (2018). Anomalously weak Labrador Sea convection and Atlantic overturning during the past 150 years. *Nature*, *556*(7700), 227–230. https://doi.org/10.1038/s41586-018-0007-4

Trouet, V., & Van Oldenborgh, G. J. (2013). KNMI Climate Explorer: A web-based research tool for high-resolution paleoclimatology. *Tree-Ring Research*, *69*(1), 3–13.

Ullman, D. J., Carlson, A. E., Anslow, F. S., LeGrande, A. N., & Licciardi, J. M. (2015). Laurentide ice-sheet instability during the last deglaciation. *Nature Geoscience*, *8*(7), 534.

van der Bilt, W. G., D'Andrea, W. J., Bakke, J., Balascio, N. L., Werner, J. P., Gjerde, M., & Bradley, R. S. (2016). Alkenone-based reconstructions reveal four-phase Holocene temperature evolution for High Arctic Svalbard. *Quaternary Science Reviews*, *183*, 204–213.

van der Bilt, W. G. M., Bakke, J., Vasskog, K., D'Andrea, W. J., Bradley, R. S., & Ólafsdóttir, S. (2015). Reconstruction of glacier variability from lake sediments reveals dynamic Holocene climate in Svalbard. *Quaternary Science Reviews*, *126*, 201–218. http://www.sciencedirect.com/science/article/pii/S0277379115301025

Werner, K., Müller, J., Husum, K., Spielhagen, R. F., Kandiano, E. S., & Polyak, L. (2015). Holocene sea subsurface and surface water masses in the Fram Strait–Comparisons of temperature and sea-ice reconstructions. *Quaternary Science Reviews*, *147*, 194–209.

Yu, S.-Y., Colman, S. M., Lowell, T. V., Milne, G. A., Fisher, T. G., Breckenridge, A., et al. (2010). Freshwater outburst from Lake Superior as a trigger for the cold event 9300 years ago. *Science*, *328*(5983), 1262–1266. https://doi.org/10.1126/science.1187860

Zhang, Y., Renssen, H., & Seppä, H. (2016). Effects of melting ice sheets and orbital forcing on the early Holocene warming in the extra-tropical Northern Hemisphere. *Climate of the Past*, *12*(5), 1119–1135. http://www.clim-past.net/12/1119/2016/

Zhang, Y., Renssen, H., Seppä, H., & Valdes, P. J. (2018). Holocene temperature trends in the extratropical Northern Hemisphere based on inter-model comparisons. *Journal of Quaternary Science*, *33*(4), 464–476.